Parallel Grid-Forming Inverter-Driven Black Start: Power-Hardware-in-the-Loop Validation

Preprint

Gab-Su Seo, Jay Sawant, and Fei Ding

National Renewable Energy Laboratory

To be presented at the 2024 Conference on Innovative Smart Grid Technologies North America (ISGT NA)
Washington, D.C.
February 19–22, 2024

NREL is a national laboratory of the U.S. Department of Energy
Office of Energy Efficiency & Renewable Energy
Operated by the Alliance for Sustainable Energy, LLC

This report is available at no cost from the National Renewable Energy Laboratory (NREL) at www.nrel.gov/publications.

Contract No. DE-AC36-08GO28308

Conference Paper
NREL/CP-5D00-87257
November 2023

Parallel Grid-Forming Inverter-Driven Black Start: Power-Hardware-in-the-Loop Validation

Preprint

Gab-Su Seo, Jay Sawant, and Fei Ding

National Renewable Energy Laboratory

Suggested Citation
Seo, Gab-Su, Jay Sawant, and Fei Ding. 2023. *Parallel Grid-Forming Inverter-Driven Black Start: Power-Hardware-in-the-Loop Validation: Preprint*. Golden, CO: National Renewable Energy Laboratory. NREL/CP-5D00-87257.
https://www.nrel.gov/docs/fy24osti/87257.pdf.

NREL is a national laboratory of the U.S. Department of Energy
Office of Energy Efficiency & Renewable Energy
Operated by the Alliance for Sustainable Energy, LLC

This report is available at no cost from the National Renewable Energy Laboratory (NREL) at www.nrel.gov/publications.

Contract No. DE-AC36-08GO28308

Conference Paper
NREL/CP-5D00-87257
November 2023

National Renewable Energy Laboratory
15013 Denver West Parkway
Golden, CO 80401
303-275-3000 • www.nrel.gov

NOTICE

This work was authored by the National Renewable Energy Laboratory, operated by Alliance for Sustainable Energy, LLC, for the U.S. Department of Energy (DOE) under Contract No. DE-AC36-08GO28308. Funding provided by U.S. Department of Energy Office of Energy Efficiency and Renewable Energy Solar Energy Technologies Office award numbers 37770 and 38637. The views expressed herein do not necessarily represent the views of the DOE or the U.S. Government.

Parallel Grid-Forming Inverter-Driven Black Start: Power-Hardware-in-the-loop Validation

Gab-Su Seo†, Jay Sawant, and Fei Ding
Power Systems Engineering Center, National Renewable Energy Laboratory, Golden, CO 80401, USA
e-mails: {gabsu.seo, jay.sawant, fei.ding}@nrel.gov

***Abstract*—With power systems encountering increasing deployment levels of inverter-based resources (IBRs), system restoration using grid-forming (GFM) IBRs has gained attention. Engineered to establish grid voltages in the absence of a stiff grid, black-start-capable GFM IBRs are expected to enhance power system resilience by playing a critical role in bottom-up system restoration. This paper experimentally studies the feasibility of the novel approach through power-hardware-in-the-loop (PHIL) testing and validation with a commercial GFM inverter. The PHIL test setup demonstrates an inverter-driven black start of a 5-MW unbalanced distribution feeder where two GFM inverters collectively black start the feeder: one is a commercial hardware GFM inverter interacting through the PHIL interface, and the other is a software GFM inverter emulated by a real-time simulation with full electromagnetic transient (EMT) models. Both GFM inverters are equipped with negative-sequence voltage control to suppress the voltage imbalance resulting from the unbalanced loading, allowing us to study the dynamic interactions between the GFM inverters with their control parameters unknown. To evaluate the dynamic behavior of the GFM inverters under the entire black-start process, the EMT model of the distribution system details the transformer and motor dynamics to emulate their inrush and startup behaviors. It abstracts conventional grid-connected inverter dynamics, i.e., grid-following inverters. Oscilloscope measurements of the hardware GFM inverter are also presented for critical steps. Takeaways for further study and field deployment are provided.**

***Index Terms*—Inverter collective black start, grid-forming inverter, inverter-based resource, negative-sequence control, power-hardware-in-the-loop validation, system restoration.**

I. Introduction

Recently, the increasing deployment levels of inverter-based resources (IBRs)—such as photovoltaics (PV), wind, and energy storage—have drawn attention because of their potential to provide black-start services. These services can include inverters as black-start resources for distribution or transmission systems or as kick-starters for large power plants [1]–[5]. Specially designed grid-forming (GFM) inverters are required to establish grid voltages without a preformed voltage from the bulk power system and to maintain stable operation with marginal capacity in the absence of other generators against extreme disturbances or off-nominal operations that could cause instability during a black start. To improve the dynamic performance of GFM inverters under nonideal conditions, advanced GFM controls have been proposed, such as advanced current limiters to improve overcurrent operation [6], [7] and dual synchronous frame control to improve power quality under unbalanced loading [8]. Due to their zero-delay startup capability and superior, programmable dynamic performance, in contrast to conventional synchronous generators, GFM IBRs located near loads can swiftly black start a power system, enhancing grid resilience [9].

IBR-driven black starts can increase the value of GFM inverters to system operators since they can fulfill multiple functions in low-inertia power systems [10], [11]. To realize an IBR-driven black start, it is critical to study solutions to overcome the technical challenges that arise from the fundamental differences between IBRs and synchronous machines. Key challenges include ensuring robust controls against dynamic load excursions that can trigger inverter overcurrents, such as motor or transformer inrush or cold-load pickup [12], as well as the reliable parallel operation of multiple GFM IBRs, which is likely required to restore a sizable system [1], among many others [3], [5]. Moreover, based on the technology development, engineering advanced GFM inverter controls with hardware and field validations in practical settings is a prerequisite for field deployment. Since black starts involve real-world power systems with a variety of uncertainties, it is paramount to validate new technologies in realistic testing environments [13].

This paper studies the GFM IBR-driven black start with rigorous hardware testing using a power-hardware-in-the-loop (PHIL) interface. The PHIL testing environment allows for evaluating the feasibility of an unbalanced distribution system black start in a realistic and complex setup using multiple GFM inverters. This yields confirming test results since it can evaluate the expected dynamic behavior of the hardware GFM inverter in a large system. For the PHIL testing, we use a recently proposed dynamic coupling method [14]. By coupling the terminal voltage dynamics of the hardware GFM inverter with proprietary advanced controls to the real-time simulation through a high-fidelity current amplifier, this work evaluates the feasibility of the parallel GFM inverter-driven black start for an unbalanced distribution system. To study its scalability and multiple, parallel GFM inverter operation, the testing scenario includes two GFM inverters: one commercial hardware and the other via software emulation. This allows for evaluating the collective GFM inverter performance for a black start, including synchronization, load pickup, and interaction

This work was authored by the National Renewable Energy Laboratory, operated by Alliance for Sustainable Energy, LLC, for the U.S. Department of Energy (DOE) under Contract No. DE-AC36-08GO28308. Funding provided by U.S. Department of Energy Office of Energy Efficiency and Renewable Energy Solar Energy Technologies Office award numbers 37770 and 38637.

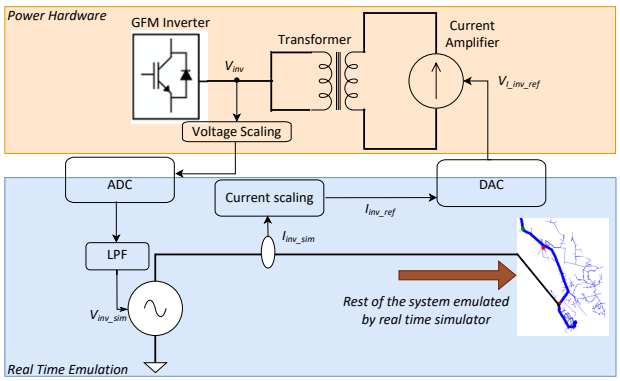

Fig. 1: PHIL setup for interfacing the hardware inverter with the RTDS simulator [14].

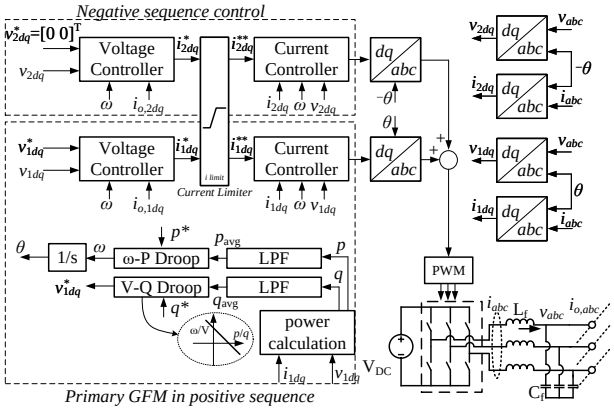

Fig. 2: GFM inverter control with negative-sequence voltage compensation [1].

with grid-following (GFL) sources. The PHIL experimental results of the black-start testing are discussed, along with key takeaways.

II. Power-Hardware-in-the-Loop Test Environment for IBR-Driven Black-Start Study

This section describes the PHIL setup, the modeling details of the GFM and GFL inverters, and the system modeling.

A. PHIL Setup

This work studies the parallel GFM inverter-driven black start of a distribution feeder using a PHIL interface. It allows for testing and validating the power hardware devices in realistic operation scenarios. For the stringent evaluation of the feasibility of the black-start concept based on GFM IBRs, the dynamics of a commercial GFM inverter hardware are coupled with the distribution feeder by using a real-time simulator that includes a software GFM inverter model and other dynamic components through the PHIL. Reliable, high-fidelity dynamic coupling is critical to yield confirming outcomes. The GFM inverter is expected to operate as a voltage source to regulate the system voltage and frequency against disturbances throughout the black-start process. This is in contrast to conventional grid-connected inverter operation, which behaves as a current source and causes challenges in setting up a reliable PHIL setup. An accurate voltage source-based representation should be modeled to capture the system dynamics when the GFM inverter interacts with the distribution network. On the other hand, the PHIL interface should represent the equivalent network (net load) seen by the GFM inverter from its terminals.

Building on the recent work reported in [14], in this paper, we implement the PHIL interface by using a voltage source-based model and a current amplifier, as shown in Fig. 1. As illustrated, the controlled voltage source in the model, V_{inv_sim}, reflects the GFM inverter terminal voltage measured, V_{inv}, and, in turn, the current observed in the model, I_{inv_sim}, which represents the rest of the distribution system, is realized by the current amplifier, I_{inv_ref}, to interact with the hardware GFM inverter under test. As illustrated, the voltage and current signals can be scaled to match the difference between the hardware and model ratings, which increases flexibility in the testing. To improve reliability, additional signal processing blocks have been added to the closed-loop system and have been validated. This PHIL setup does not require internal inverter control parameter information, which is likely proprietary to the inverter manufacturers, i.e., it is a black-box approach, which eases testing commercial hardware. For parallel GFM inverter operation testing and performance estimates, the steady-state and dynamic characteristics of the hardware inverter, such as P-f and Q-V droop gains, can be measured and used for coordination, e.g., power sharing among GFM assets.

B. GFM Inverters

The control architecture of the emulated GFM inverter is shown in Fig. 2. It employs the classical droop control with voltage and current control loops cascaded in the dq reference frame. Notable is the negative-sequence control to balance the phase voltages because distribution feeders are unbalanced. The negative-sequence control used in this study has voltage and current control loops, as shown in Fig. 2, based on the work found in [8]. As illustrated, the GFM control can be equipped with a phase current limiter for asymmetrical overloading. Ideally, the negative-sequence compensation should be shared among capable resources; more study on this topic is necessary to ensure power quality, stability, and interoperability [11]. Whether the hardware GFM inverter is equipped with the voltage balancing control and its type is unknown; this will be investigated with the black-box approach.

C. IBR Interconnection and Load Transformers

To evaluate the GFM inverter performance in the transformer energization, we model the saturation and hysteresis of the three-phase and single-phase transformers. The magnetizing current is included as part of the saturation. The grid interconnection transformer, which connects the software GFM inverter to the medium-voltage grid, is modeled in the $\Delta - Y_g$ configuration (0.48-kV Δ to 24.95-kV Y_g) to form a reliable grounding source for the islanded microgrids in the absence of a substation [15]. The same applies to the controllable voltage source, which represents the hardware

TABLE I: GFM Inverter Specifications: GFM 1 (top, SW) and GFM 2 (bottom, HW).

Item	Design Selections
Inverter parameters	P_{rated} = 2.5 MW, V_{rated} = 277/480 V, L_{f} = 0.15 p.u., C_{f} = 5 p.u.
Inner-loop control	$k^{\text{P}}_{\text{V1C}}$ = 1, $k^{\text{i}}_{\text{V1C}}$ = 3, $k^{\text{P}}_{\text{I1C}}$ = 0.73, $k^{\text{i}}_{\text{I1C}}$ = 1.19, $k^{\text{P}}_{\text{V2C}}$ = 1, $k^{\text{i}}_{\text{V2C}}$ = 5 $k^{\text{i}}_{\text{I2C}}$ = 0.35, $k^{\text{P}}_{\text{I2C}}$ = 0.5
Droop	k_p = 0.006, k_q = 0.1, ω_{n} = $2\pi \cdot 60$ rad/sec
Inverter	P_{rated} = 30 kVA, V_{rated} = 277/480 V
Droop (hardware - measured)	k_p = 0.006, k_q = 0.1

TABLE II: Test Feeder Power Flow and GFL DER Information per Breaker Segment.

Location	Power Flow (P and Q)	DER Capacity
B7	250 kW, 200 kVar	50 kW
B8	75 kW, 20 kVar	40 kW
B9	470 kW, 300 kVar	150 kW
B10	250 kW, 150 kVar	200 kW
B11	250 kW, 125 kVar	200 kW
B12	230 kW, 150 kVar	150 kW
B13	800 kW, 400 kVar	250 kW

inverter in the model; it is interconnected with the $\Delta - Y_g$ transformer.

D. Loads

Loads are modeled as dynamic RL loads. Each load emulates a constant impedance when the terminal voltage are less than 0.8 p.u., whereas for voltages greater than 0.8 p.u., the load emulates a constant power load. This is to accurately capture the voltage-dependant load behavior during the inverter-driven black start, which could experience off-nominal voltages due to overloading. During the black start, loads can be shed depending on their criticality, which decreases the GFM inverter capacity required.

E. Induction Motors

A three-phase induction motor is modeled to study the dynamics of the direct online motor start in the black start. The motor model is equipped with a stator-side breaker to simulate the direct-starting process [16].

F. GFL Distributed Energy Resources

In this paper, behind-the-meter distributed energy resources (DERs) are modeled as equivalent current sources. The dynamics of the phase-locked loop and power and current control loops are considered in the model, with their DC-side assumed to be tightly regulated [17]. The real and reactive power set points to the DERs are set to the power available in the test scenario and zero, respectively. To aid the black-start process, the GFL DERs are programmed to turn on 2 s after their terminal voltages reach the normal value. Additionally, to provide voltage support functionality, a utility-scale GFL IBR is configured to inject reactive power.

III. Black-Start Test Scenario and Results

A. Feeder Model and Critical Model Details

Fig. 3(a) shows the 5-MVA distribution feeder for this study with two utility-scale GFM IBRs. Both GFM IBRs are used

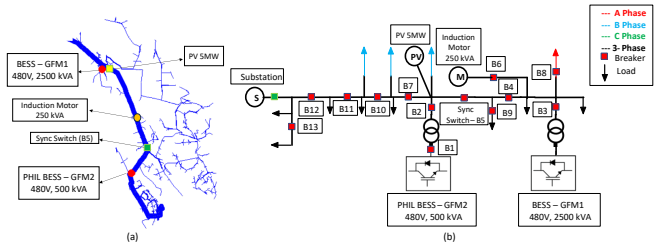

Fig. 3: Feeder for validation: (a) model abstracted and (b) simplified network diagram.

to evaluate the parallel inverter-driven black start: $GFM1$, rated at 2.5 MVA, is software emulated, and $GFM2$, scaled at 0.5 MVA, is coupled with the hardware GFM IBRs. A battery energy storage system (BESS) powers the GFM IBRs. In addition, one 5-MVA utility-scale PV plant is located near $GFM1$ to support the reactive power. The test feeder is constructed based on a real distribution network in western Colorado. Table I lists the GFM inverter parameters. The droop gains are measured for the hardware inverter, $GFM2$, with the default control settings. As discussed in Section II, the current signal is scaled to match the difference in the rating for $GFM2$.

Fig. 3(b) shows the simplified electrical diagram of the entire feeder under study. Upon an outage, the distribution system operator checks the system status, including points of failure and breaker status. Once safety and readiness are assured, $GFM1$ and $GFM2$ initiate the black start, forming local microgrids and independently recovering the backbone. Once they reach the boundary, the synchronization switch, $B5$, merges the two grids, which allows the two GFM IBRs to collectively recover the rest of the system using breakers ($B6$–$B15$). Each segment, which is separated by the breakers in the feeder, has its own set of local loads, residential transformers, and GFL DERs, as tabulated in Table II. One 250-kVA, three-phase induction motor that represents the motor loads of the entire feeder, the GFL DERs that automatically turn on and support the power generation, and the three-phase and single-phase residential transformers and loads are not detailed in the diagram. To reduce the GFM IBR capacity required for the black start, this work sheds noncritical loads, at 20% of rating, and prioritizes critical loads. Details are found in Table II.

B. Test Results of Parallel GFM-Driven Black Start

This section reports the PHIL-based test results. The breaker closing sequence used for the test is as follows, based on the assumed network conditions: $B1$, $B2$&$B3$, $B4$, $B5$ (sync), $B6$ (motor), $B7$, $B8$, $B9$, $B10$, $B11$, $B12$, and $B13$. The sequence of the load recovery and merging is an important topic for future work [18].

Fig. 4 displays the test results of the entire black-start process. It shows the measurements of the GFM IBR voltages, currents, real and reactive power, and inverter frequencies, with the breaker closing-associated transients noted. As shown, the GFL DERs automatically participate in the black-start process by providing real power support as their terminal voltages recover, which increases the headroom of the GFM

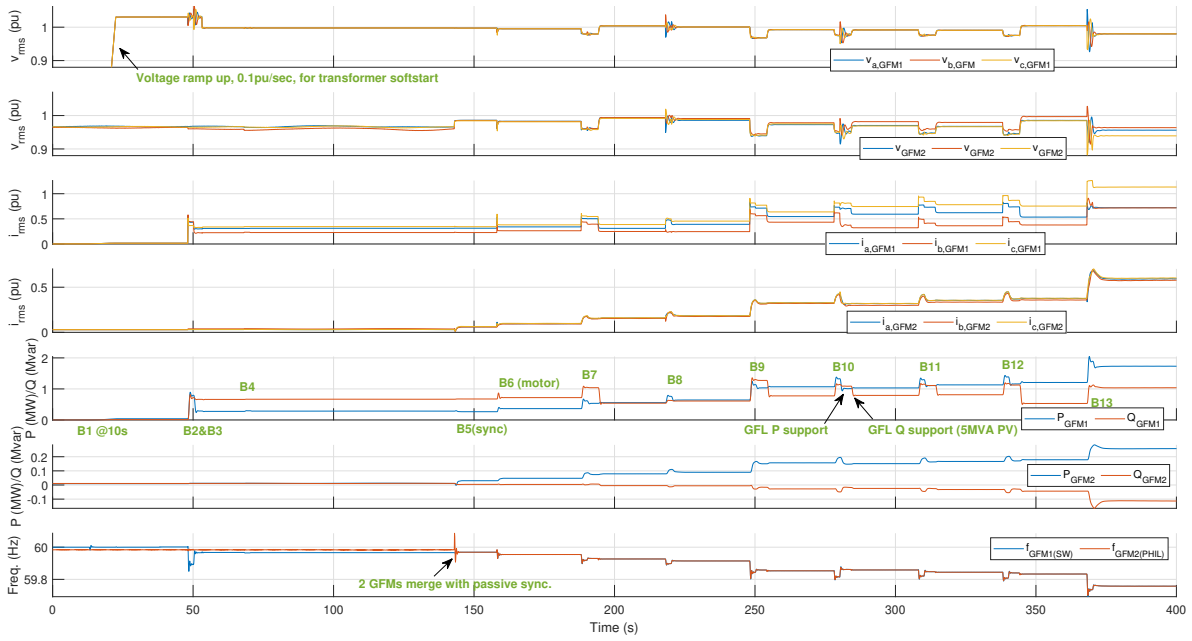

Fig. 4: Entire test results: two GFM inverters, one in simulation and the other in hardware, collectively black start the 5-MVA feeder.

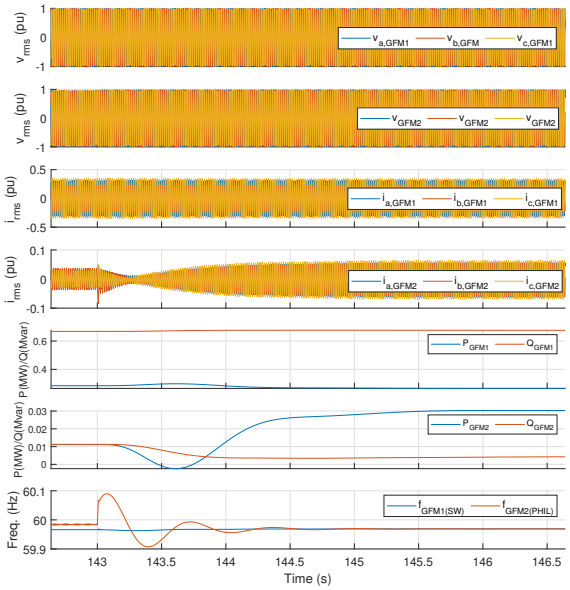

Fig. 5: Synchronization ($B5$) of the two GFM inverters, with one in PHIL coupling.

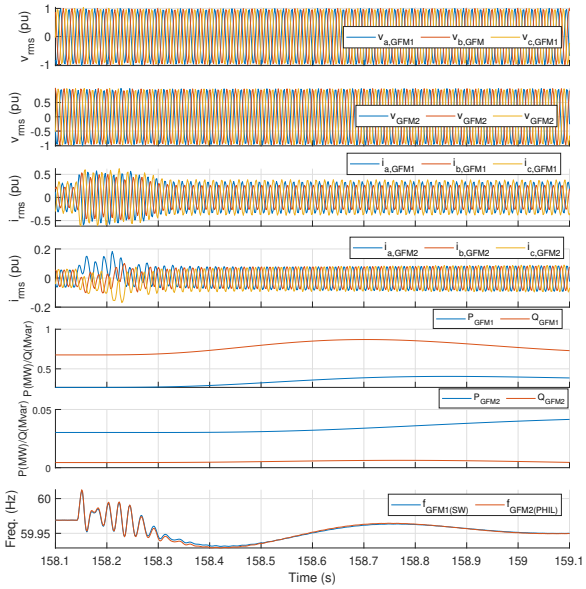

Fig. 6: Two GFM IBRs start the 250-kVA induction motor.

inverters [1]. The 5-MVA PV plant, on the other hand, injects reactive power, by an open-loop control, to support the system voltage when the feeder voltage dips below 0.9 p.u. The utilization of different inverter assets can vary and is critical for a successful black start.

Due to the space limit, only key transients are discussed in detail. Fig. 5 zooms in on the synchronization transients by $B5$. After the initial transients, for a short duration, the oscillations damp out, and the resultant network reaches a stable operating point. The droop-controlled GFM IBR-sourced networks have been known to reliably merge; however, a successful microgrid merging of GFM IBRs with negative-sequence voltage compensation coupled with PHIL interface is noteworthy. It underlines the potential of a successful black start and grid operation driven by IBRs of different underlying controls, likely proprietary, with minimal coordination, such as steady-state power sharing by droop characteristics, which are readily available. More research in this space is necessary to develop interoperability standards covering the steady-state and fault/overloading behavior of GFM IBRs.

Fig. 6 shows the 250-kVA induction motor start transient ($B6$). The two GFM IBRs, now merged, provide the high reactive power required for starting the induction motor. Note that the currents provided during the transient differ between the two GFM IBRs because of the difference in their power ratings, 5:1, and the location of the motor near $GFM1$. Fig. 7 highlights the last load recovery by closing $B13$. As shown, even with the unbalanced loading, the inverter terminal

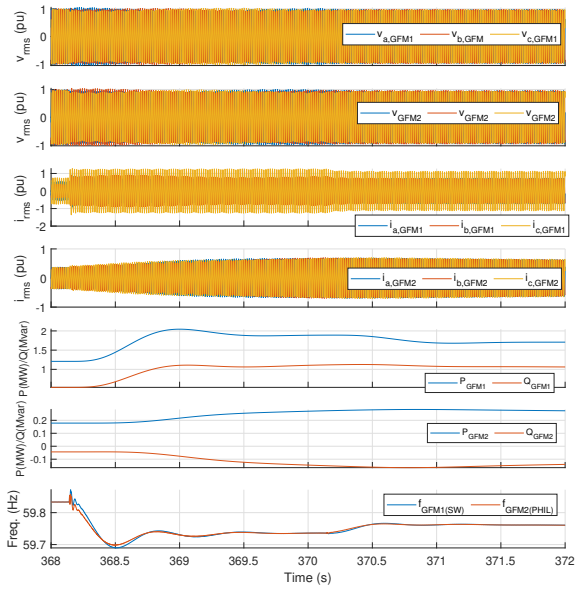

Fig. 7: Final load pickup ($B13$) followed by the GFL DER active power support.

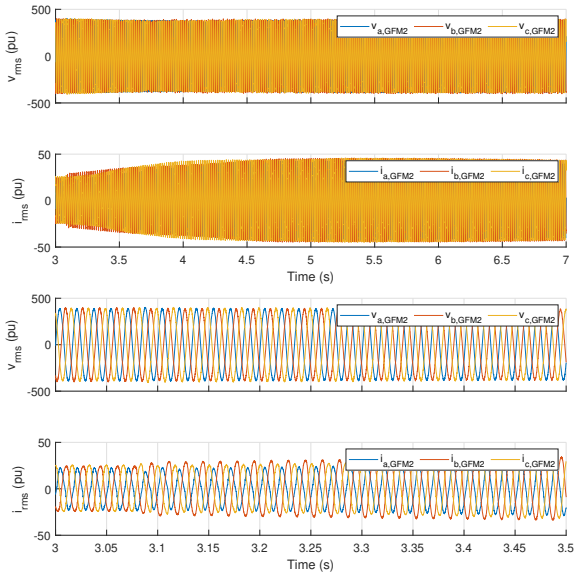

Fig. 8: Oscilloscope measurements of the hardware GFM inverter under the last load pickup followed by the 250-kW GFL DERs. Voltages and currents at the bottom detail the load response. This time stamp does not match those of the other figures.

voltages remain balanced by the negative-sequence control of $GFM1$ after a momentary imbalance resulting from the unbalanced load transient (also noticeable in Fig. 4). Fig. 7 also shows the GFL DER operation. Near $t = 370.2\ s$, the GFL DERs under $B13$ inject active power, $2\ s$ after their terminal voltages return to normal. As discussed, if properly configured, the GFL support would help reduce the GFM IBR capacity requirements for a successful black start.

IV. Conclusions and Future Work

This paper has experimentally evaluated a parallel GFM IBR-driven black start through PHIL-based testing and validation. It used a commercial hardware GFM inverter to black start a 5-MVA real-world distribution feeder that is emulated by a real-time simulator. The high-fidelity coupling of the power hardware device with the detailed real-time simulation allowed for evaluating the dynamic system restoration process using advanced GFM inverters with supplementary controls, including negative-sequence voltage compensation that is compatible with parallel GFM operation, which are critical to ensure a resilient black start and power quality. Test results of the hardware GFM with unknown underlying control parameters imply the feasibility of a successful black start and grid operation of IBRs from different vendors with minimal coordination. This needs further investigation and will influence interoperability standard development. Future work includes continued evaluation with different scenarios, including corner cases, testing with more hardware devices (both GFM and GFL), black-start sequence optimization with intelligence, and field demonstrations.

References

[1] J. Sawant, G.-S. Seo, and F. Ding, "Resilient inverter-driven black start with collective parallel grid-forming operation," in *Proc. IEEE Innovative Smart Grid Tech. Conf.*, pp. 1–5, 2023.

[2] A. Jain, J. N. Sakamuri, and N. A. Cutululis, "Grid-forming control strategies for black start by offshore wind power plants," *Wind Energy Science*, vol. 5, no. 4, pp. 1297–1313, 2020.

[3] H. Jain, G.-S. Seo, E. Lockhart, V. Gevorgian, and B. Kroposki, "Blackstart of power grids with inverter-based resources," in *IEEE Power & Energy Society General Meeting*, pp. 1–5, 2020.

[4] S. Li, M. Zhou, Z. Liu, J. Zhang, and Y. Li, "A study on vsc-hvdc based black start compared with traditional black start," in *IEEE International conference on sustainable power generation and supply*, pp. 1–6, 2009.

[5] B.-M. S. Hodge *et al.*, "Addressing technical challenges in 100% variable inverter-based renewable energy power systems," *Wiley Interdiscip. Rev. Energy Environ.*, vol. 9, no. 5, p. e376, 2020.

[6] N. Baeckeland and G.-S. Seo, "Novel hybrid current limiter for grid-forming inverter control during unbalanced faults," in *International Conference on Power Electronics-ECCE Asia*, pp. 1517–1522, 2023.

[7] N. Baeckeland and G.-S. Seo, "Frequency synchronization of grid-forming inverters under fault conditions and overloading," in *Proc. IEEE Workshop Control Modelling Power Electron.*, pp. 1–8, 2023.

[8] B. Mahamedi, M. Eskandari, J. E. Fletcher, and J. Zhu, "Sequence-based control strategy with current limiting for the fault ride-through of inverter-interfaced distributed generators," *IEEE Transactions on Sustainable Energy*, vol. 11, no. 1, pp. 165–174, 2018.

[9] G.-S. Seo, J. Sawant, and F. Ding, "Black start of unbalanced microgrids harmonizing single- and three-phase grid-forming inverters," in *IEEE Power & Energy Society General Meeting*, pp. 1–6, 2023.

[10] Y. Lin *et al.*, "Research roadmap on grid-forming inverters," tech. rep., National Renewable Energy Lab., Golden, CO (United States), 2020.

[11] D. Ramasubramanian et al., "Performance specifications for grid-forming technologies," in *IEEE Power & Energy Soc. Gen. Meet.*, pp. 1–6, 2023.

[12] H. Chang, N. Baeckeland, A. Banerjee, and G.-S. Seo, "Universal passive synchronization method for grid-forming inverters without mode transition," in *ECCE Asia*, pp. 1523–1529, 2023.

[13] H. Burroughs, C. Klauber, C.-C. Sun, and M. J. Culler, "Black start with inverter-based resources: Hardware testing," in *IEEE Power & Energy Society General Meeting*, pp. 1–6, 2023.

[14] A. Pratt, K. Prabakar, S. Ganguly, and S. Tiwari, "Power hardware-in-the-loop interfaces for inverter-based microgrid experiments including transitions," in *IEEE ECCE*, p. to be presented, 2023.

[15] A. Vukojevic and S. Lukic, "Microgrid protection and control schemes for seamless transition to island and grid synchronization," *IEEE Transactions on Smart Grid*, vol. 11, no. 4, pp. 2845–2855, 2020.

[16] S.-K. Sul, *Control of electric machine drive systems*. John Wiley & Sons, 2011.

[17] A. Yazdani and R. Iravani, *Voltage-sourced converters in power systems: modeling, control, and applications*. John Wiley & Sons, 2010.

[18] E. Fix, A. Banerjee, U. Muenz, and G.-S. Seo, "Investigating multi-microgrid black start methods using grid forming inverters," in *Proc. IEEE Innovative Smart Grid Tech. Conf.*, pp. 1–5, 2023.